Supplementary information for
Ecological and societal effects of Central Asian streamflow variations over the past eight centuries

Feng Chen[1, 2]*, Yujiang Yuan[2], Valerie Trouet[3], Ulf Büntgen[4], Jan Esper[5], Fahu Chen[6, 7]*, Shulong Yu[2], Miaogen Shen[8], Ruibo Zhang[2], Huaming Shang[2], Youping Chen[1, 2], Heli Zhang[2]

1. Yunnan Key Laboratory of International Rivers and Transboundary Eco-Security, Institute of International Rivers and Eco-Security, Yunnan University, Kunming, China

2. Key Laboratory of Tree-ring Physical and Chemical Research of China Meteorological Administration/Xinjiang Laboratory of Tree-ring Ecology, Institute of Desert Meteorology, China Meteorological Administration, Urumqi, China

3. Laboratory of Tree-Ring Research, University of Arizona, Tucson, Arizona, USA

4. Department of Geography, University of Cambridge, Cambridge, UK

5. Department of Geography, Johannes Gutenberg University, Mainz, Germany

6. Key Laboratory of Alpine Ecology, CAS Center for Excellence in Tibetan Plateau Earth Sciences and Institute of Tibetan Plateau Research, Chinese Academy of Sciences (CAS), Beijing, China.

7. Key Laboratory of Western China's Environmental Systems (Ministry of Education), College of Earth and Environmental Sciences, Lanzhou University, Lanzhou, China.

8. State Key Laboratory of Earth Surface Processes and Resource Ecology, Faculty of Geographical Science, Beijing Normal University, Beijing, China

* Corresponding Authors

feng653@163.com (Feng Chen)

fhchen@itpcas.ac.cn (Fahu Chen)

Data and methods

Tree-ring data

The study area is located in Tien Shan, China and Kyrgyzstan, which is the source area of many major Central Asian rivers, such as the Syr Darya, Ili, and Chu rivers (Fig. 1 and Supplementary Fig. 1). Pristine stands of Schrenk spruce growing at two water-stressed sites (JPK and XHZ) distributed over an elevation range of 2215–2500 m a.s.l. were sampled at the Ebinur Lake Basin, which is the largest salt lake in Xinjiang, in 2005 and 2010 (Supplementary Table 1). Generally, Schrenk spruce trees prefer to colonize wet settings with deep soil and form open canopy forests on sunny slopes and at the tree line. In the open and dry stands of the Tien Shan, the competition among trees is relatively low and the spruce trees are sensitive to moisture availability (Supplementary Fig. 2). Two increment core samples were collected from each tree. In combination, the two sites in China provide 258 samples from 140 trees. After mounting and sanding, annual tree-ring widths were measured to the nearest 0.001 mm and cross-dated using COFECHA software [1]. In addition, tree-ring width data from two sites (ENG and KOE) in Tien Shan, Kyrgyzstan were obtained from the International Tree Ring Data Bank (ITRDB, http://www.ncdc.noaa.gov/data-access/paleoclimatologydata/datasets/tree-ring) [2]. Conservative detrending methods (negative exponential curve fits) were applied using the software ARSTAN to develop standard tree-ring width chronologies that retain low values through high-frequency common signals [3]. An RBAR-weighted method was used to stabilize the variance of the tree-ring chronologies [4]. Significantly positive correlations between the Kyrgyzstan and Chinese chronologies ($r = 0.35$, n = 665, $p < 0.01$) indicated that the series contains a common signal (Supplementary Fig. 3); thus, we combined all series of the four sites into a composite chronology. The mean tree age is 304 years, and the average annual growth rate is 0.24 mm. High mean sensitivity (MS), standard deviation (SD), and signal to noise ratio (SNR) values indicate strong climatic influence on tree growth (Supplementary Table 1). The RBAR (mean correlation between ring-width series) and expressed population signal (EPS) used 50-year windows with a lag of 25 years to evaluate the adequacy of replication in the early years of the chronology [5]. We truncated the composite chronology at the year 1225 CE based on the EPS value of 0.85, when sample depth dropped below six series from three trees.

Streamflow data and statistical analysis

The correlation analyses between our composite chronology and the hydroclimatic/NDVI data [6, 7] were performed using the software DENDROCLIM2002 [8]. Monthly hydroclimatic data for a window from July of the previous year to October of the current year were used in the correlation analyses. We used the composite chronology as the predictor and the instrumental annual (August-July) streamflow sum of the four rivers as the predictand in a simple linear regression to develop a streamflow reconstruction for the past 785 years. To assess the reliability of the reconstruction model, a leave-one-out cross-validation method [9] was applied for the 1962-2009 period, and the reduction of error (RE), coefficient of efficiency (CE), Pearson correlation coefficient, and sign test (ST) statistics were calculated [3]. Both the RE and CE, but particularly the CE, are rigorous statistics for which any positive value indicates useful information in the reconstruction [3]. The results of the sign test, which describes how well the predicted value tracks the direction of instrumental data, exceed the 95% confidence level. We calculated the uncertainty of our streamflow reconstruction from the root mean square error (RMSE) of validation and defined high and low streamflow years as those beyond ±1 standard deviation from the mean and extremely high and low years as those beyond ±2 standard deviations.

As an important channel for human migration in Central Asia, our study area is in the vicinity of the Pre-Balkhash plague focus area of southern Kazakhstan [10]. Our reconstruction thus also reveals the role of water availability in plague outbreaks. In addition to local hydroclimatic data, we also used the KNMI Climate Explorer [11] to calculate spatial correlation maps between our streamflow reconstruction and August-October NDVI (8 km ×8 km) [6]. The gridded PDSI reconstruction for the Mediterranean Basin for 1000–2014 CE (averaged over 30–45° N, -5–37° E) was extracted from the Old World Drought Atlas [12, 13], the tree ring–based field June-August drought reconstruction. We also conducted spatial correlations between the PDSI reconstruction and the updated 0.5°× 0.5° gridded self-calibrating Palmer Drought Severity Index (scPDSI) of CRU TS3.26 [14] and NDVI. To develop a plague subset of over the Mediterranean region and Europe that linked with plague outbreaks in Asia, we selected only those plague events that followed within 5 years of a new period of plague outbreaks in Asia, using the regional datasets of plague outbreaks [10, 15, 16]. This selection procedure resulted in a shortlist of 18 plague events in the Mediterranean region and Europe: 1346, 1408, 1409, 1575, 1630, 1647, 1689, 1691, 1719, 1736, 1757, 1760, 1770, 1780, 1783, 1828, 1830 and 1833 (Supplementary Table S2). We investigated hydrologic situation in the Tien Shan during the plague event year described above using a superposed epoch analysis (SEA, https://rdrr.io/cran/dplR/man/sea.html) [17]. We tested significance using modified block reshuffling to evaluate the significance of autocorrelations in the streamflow reconstruction. Meanwhile, for Granger causality analysis [18], plague data of the same outbreak year in Europe in 1347–1830 CE are aggregated together to form a time series based on the geo-referenced historical plague database [19]. In our case, we say that *x* Granger causes *y* if future values of *y* can be better projected using the past values of *x* and *y* rather than just past values of *y*. Thus, we can develop an autoregressive (AR) equation of order k -AR(k) - using only y values, a vector autoregressive (VAR) equation of the same order-VAR(k)-using both x and y values and assess their predict performance on some tests, include the MSE-t test and the MSE-REG test, in terms of mean square error (MSE) [20, 21]. The significant level was set at 0.1 and 0.05. Based on the results of SEA analysis and GCA analysis, we can reveal the hydrologic situation in Central Asia before and after the outbreak of the plague, and reveal the possible influence of the streamflow condition on the plague. Multi-taper method (MTM) of spectral analysis [22] was used to summarize the cycles of the streamflow reconstruction.

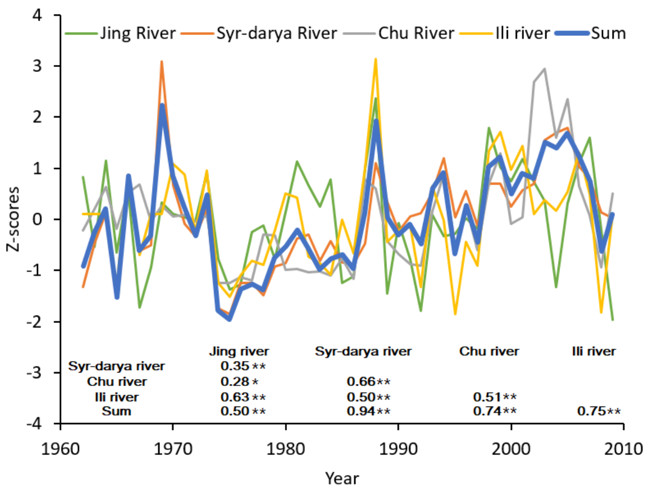

Supplementary Figure 1: Graphical comparison of annual streamflow of the Syr-Darya, Ili, Chu, and Jing rivers. ** Significant at $p < 0.01$; * significant at $p < 0.05$.

Supplementary Figure 2: Dry sampling site (JPK) within the Tien Shan near the Ebinur lake basin characterized by open spruce forests and wide talus slopes.

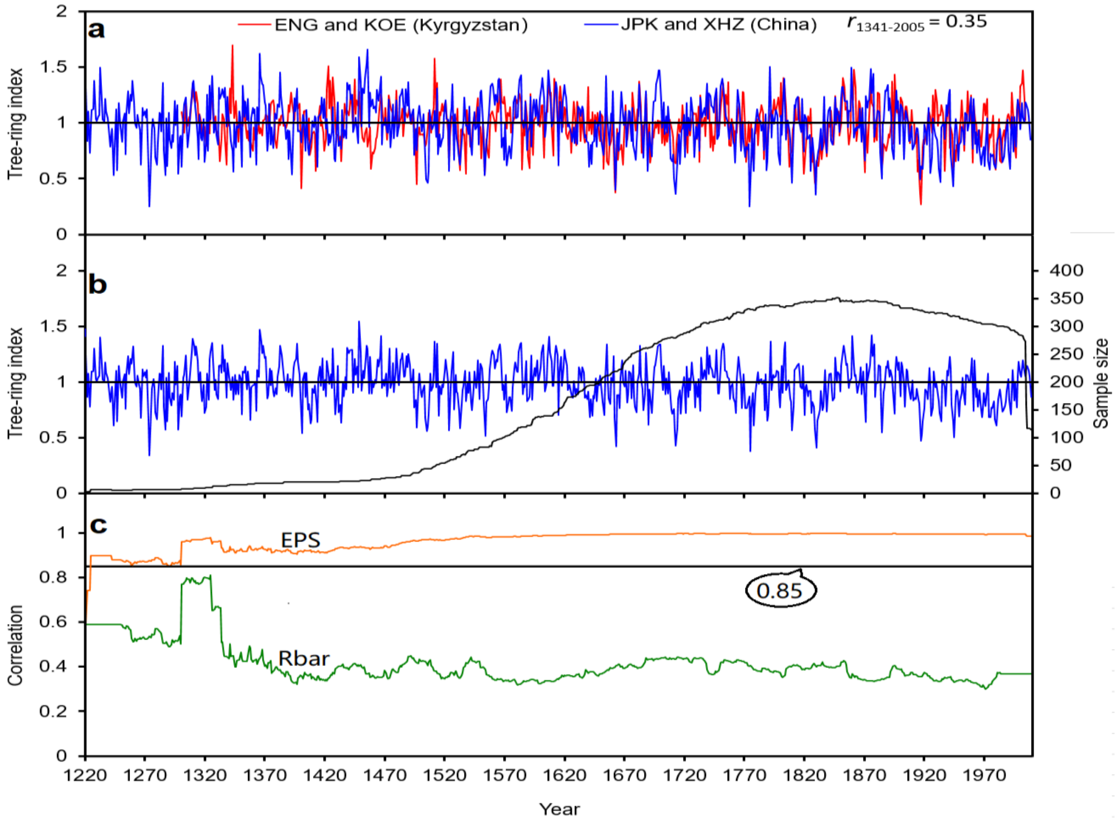

Supplementary Figure 3: (a) Comparison between the tree-ring width chronologies of Tien Shan, Kyrgyzstan (ENG and KOE, red curve) and China (XHZ and JPK, blue). (b) Composite chronology (blue) and underlying sample replication (black), and (c) the EPS (red) and RBAR (green) statistics of the regional chronology from 1220–2009 CE. The horizontal line denotes the 0.85 EPS value for signal strength acceptance.

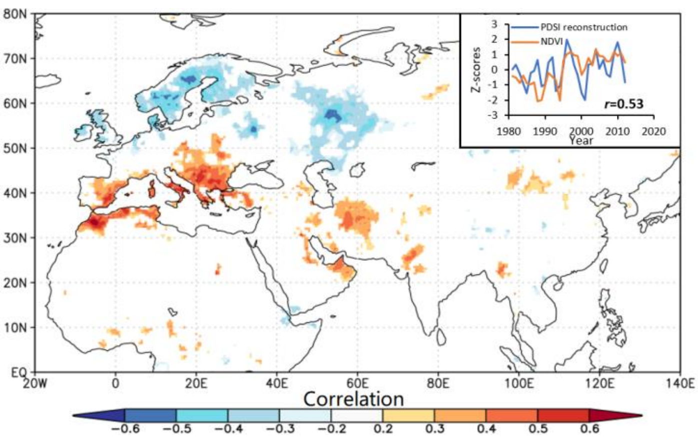

Supplementary Figure 4: Correlation patterns of the PDSI reconstruction [12] withinstrumental June-August PDSI over their period of overlap (1950-2012). Insignificant correlations ($p > 0.05$) are masked out. Image in the upper right corner indicates the comparison between the PDSI reconstruction and mean July-September NDVI for 1981 to 2012.

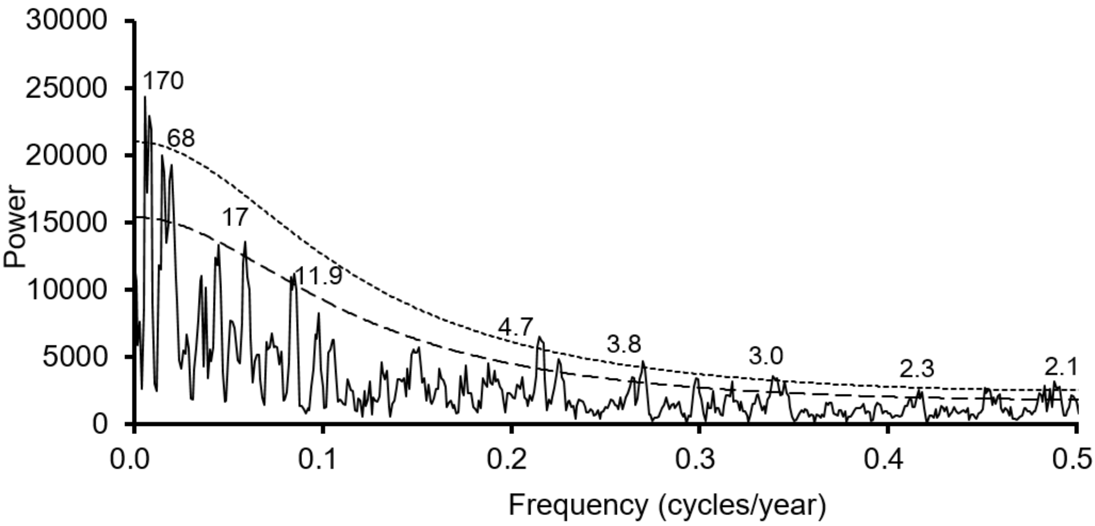

Supplementary Figure 5: MTM spectral density of the streamflow reconstruction. The dash and dotted lines indicate the 95% and 99% significance level, respectively.

Supplementary Table 1: Site information and descriptive statistics for the tree-ring chronologies. Locations of the corresponding hydrological stations in Central Asia are found in Fig. 1a.

Country	Site	Lat. (N)	Long. (E)	Elevation (m a.l.s.)	Core /Tree number	Length	MS	SD	SNR	EPS	Annual Streamflow (10^8 m^3)
China	JPK	44°06′	82°54′	2270-2500	202/112	1217-2009					
	XHZ	44°22′	83°15′	2215-2400	56/28	1594-2009					
					258/140	1217-2009	0.20	0.23	88.32	0.99	
Kyrgyzstan	ENG	42°09′	79°28′	2950	99/50	1301-2005					
	KOE	42°09′	79°28′	2827	39/20	1450-2005					
					138/70	1301-2005	0.17	0.19	49.78	0.98	
	Composite chronology				396/210	1217-2009	0.17	0.19	118.92	0.99	
China	Jinghe (Jing river)	44°22′	82°55′	619		1962-2009					4.7
Kazakhstan	Chapaevo (Chu river)	43°25′	73°54′	320		1962-2009					20.0
Tajikistan	Akdjar (Syr-Darya river)	40°40′	70°43′	365		1962-2009					169.5
Kazakhstan	Ushjarma (Ili river)	45°03′	75°27′	390		1962-2009					145.7

Note: MS is the mean sensitivity; SD is the standard deviation; SNR is the signal-to noise ratio; and EPS is the expressed population signal.

Supplementary Table 2: Some plague events of the Mediterranean Basin and Europe and the streamflow values of the previous 15 years in Central Asia.

Plague events	Response year	Response streamflow (1×10^8 m^3)	Percentage	Response high streamflow years
Kaffa, Ukraine (1346)	1332 (-15 years)	401.9	12.0%	1332-1337
Barcelona, Spain (1408)	1394 (-15 years)	395.8	10.3%	1394-1399
Constantinople, Turkey (1409)	1395 (-15 years)	408.9	13.9%	1394-1399
Venice, Italy (1575)	1561 (-15 years)	427.0	19.0%	1558-1567
Milan, Italy (1630)	1616 (-15 years)	383.5	6.9%	1616-1622
Valencia, Spain (1647)	1633 (-15 years)	391.0	8.9%	1632-1636
Izmir, Turkey (1689)	1675 (-15 years)	383.2	6.8%	
Southern Russia (1691) and Alexandria, Egypt (1693)	1677 (-15 years)	403.3	12.4%	
Gdansk, Poland (1719) and Marseilles, France (1720)	1705 (-15 years)	370.7	3.3%	1694-1703
Kabarda, Russia (1736-1737) and Gdansk, Poland (1737)	1722 (-15 years)	399.3	11.3%	
Izmir, Turkey (1757)	1743 (-15 years)	391.5	9.1%	1734-1747
Tripoli, Libya (1760) and Algeria, Algeria (1762)	1746 (-15 years)	396.1	10.4%	1734-1747
Moscow, Russia (1770)	1756 (-15 years)	374.2	4.3%	1750-1757
Algeria, Algeria (1780)	1766 (-15 years)	403.3	12.4%	1764-1767
Algeria, Algeria (1783)	1769 (-15 years)	380.8	6.1%	
Tripoli, Libya (1828)	1814 (-15 years)	401.9	12.0%	1812-1816
Beirut, Lebanon (1830)	1816 (-15 years)	384.0	7.0%	1812-1816
Alexandria, Egypt (1833-1835) and Tunis, Tunisia (1837)	1819 (-15 years)	401.4	11.8%	

Supplementary Table 3: Leave-one-out cross-validation statistics for the August-July composite streamflow reconstruction for Tien Shan based on the composite chronology.

	r	RE/CE	ST
Syr-Darya, Ili, Chu and Jing river	0.66	0.67/0.34	$40^{+}/7^{-}$

Supplementary Table 4: Summary characteristics of the streamflow reconstruction in the different centuries.

Period	Mean	Standard deviation
1225-1299	355.0	52.1
1300-1399	375.7	45.5
1400-1499	369.8	51.1
1500-1599	358.5	51.3
1600-1699	362.1	50.9
1700-1799	354.1	51.3
1800-1899	360.4	52.2
1900-1999	332.0	43.2

Supplementary Table 5: Results of GCA

Null hypothesis	*F*	*P*
Streamflow does not Granger-cause plague outbreak (Lags: 14)	1.95	0.01
Streamflow does not Granger-cause plague outbreak (Lags: 15)	1.83	0.02
Streamflow does not Granger-cause plague outbreak (Lags: 16)	1.81	0.03

Supplementary References

1. Holmes, R.L. Computer-assisted quality control in tree-ring dating and measurement. *Tree-ring Bull*. **43**, 69-78 (1983).

2. PAGES 2k Consortium. Continental-scale temperature variability during the past two millennia. *Nature Geosci.* **6**, 503 (2013).

3. Cook, E. R. & Kairiukstis, L. A. Methods of Dendrochronology: Applications in the Environmental Sciences (Kluwer Academic, Dordrecht, The Netherlands, 1990).

4. Osborn, T. J., Biffa, K. R. & Jones, P. D. Adjusting variance for sample-size in tree-ring chronologies and other regional-mean timeseries. *Dendrochronologia*, **15**, 89-99 (1997).

5. Wigley, T. M. L., Briffa, K. R. & Jones, P. D. On the average value of correlated time series, with applications in dendroclimatology and hydrometeorology. *J. Clim. appl. Met.* **23**, 201–213 (1984).

6. Tucker, C. J. et al. An extended AVHRR 8-km NDVI data set compatible with MODIS and SPOT vegetation NDVI data. *Int. J. Remote Sens.* **26**, 4485–5598 (2005).

7. Harris, I. P. D. J., Jones, P. D., Osborn, T. J. & Lister, D. H. Updated high-resolution grids of monthly climatic observations-the CRU TS3. 10 Dataset. *Int. J. Climatol.* **34**, 623-642 (2014).

8. Biondi, F. & Waikul, K. DENDROCLIM2002: A C program for statistical calibration of climate signals in tree-ring chronologies. *Comput. Geosci.* **30**, 303–311 (2004).

9. Michaelsen, J. Cross-validation in statistical climate forecast models. *J. Clim. appl. Met.* **26**, 1589-1600 (1987).

10. Schmid, B. V. et al. Climate-driven introduction of the Black Death and successive plague reintroductions into Europe. *Proc. Natl Acad. Sci. USA* **112**, 3020-3025 (2015).

11. Trouet, V. & Van Oldenborgh, G. J. (2013). KNMI Climate Explorer: a web-based research tool for high-resolution paleoclimatology. *Tree-Ring Res*. **69**, 3-13.

12. Cook, E. R. et al. Old World megadroughts and pluvials during the Common Era. *Sci. Adv.* **1**, e1500561 (2015).

13. Cook, B. I., Anchukaitis, K. J., Touchan, R., Meko, D. M. & Cook, E. R. Spatiotemporal drought variability in the Mediterranean over the last 900 years. *J. Geophys. Res.: Atmos.* **121**, 2060-2074 (2016).

14. van der Schrier, G., Barichivich, J., Briffa, K. R. & Jones, P. D. A scPDSI-based global data set

of dry and wet spells for 1901-2009. *J. Geophy. Res.: Atmos.* **118**, 4025-4048 (2013).

15. Zietz, B. P. & Dunkelberg, H. The history of the plague and the research on the causative agent Yersinia pestis. *Int. J. Hyg. Envir. Heal.* **207**, 165-178 (2004).

16. Dols, M.W. The second plague pandemic and its recurrences in the Middle East: 1347-1894. *J Econ. Soc. History of the Orient* **22**,162–189 (1979).

17. Haurwitz, M. W. & Brier, G. W. A critique of superposed epoch analysis method: Its application to solar-weather relations. *Mon. Weath. Rev*. **109**, 2074–2079 (1981).

18. Granger, C. W. Some recent development in a concept of causality. *J. Econ.* **39**, 199-211 (1988).

19. Büntgen, U., Ginzler, C., Esper, J., Tegel, W. & McMichael, A. J. Digitizing historical plague. *Clin. Infect. Dis.* 55, 1586-1588 (2012).

20. Granger, C. W. J. & Newbold, P. Forecasting Economic Time Series 2nd edn. (Academic Press, San Diego, 1986)

21. McCracken, M. W. Asymptotics for out of sample tests of Granger causality. *J. Econ.* **140**, 719-752 (2007).

22. Mann, M. E. & Lees, J.M. Robust estimation of background noise and signal detection in climatic time series. *Clim. Change* 33, 409-445 (1996).